Eur. Phys. J. B **47**, 63–70 (2005)
DOI: 10.1140/epjb/e2005-00301-6

THE EUROPEAN PHYSICAL JOURNAL B

Structural, electronic and optical properties of fluorite-type compounds

R. Khenata[1,2], B. Daoudi[2], M. Sahnoun[1,a], H. Baltache[1], M. Rérat[3], A.H. Reshak[4], B. Bouhafs[5], H. Abid[2], and M. Driz[1]

[1] Laboratoire de Physique Quantique et de Modélisation Mathématique (LPQ3M), Département de Technologie, Université de Mascara, Algeria
[2] Applied Materials Laboratory (AML), Electronics Department, University of Sidi-Bel-Abbès, Algeria
[3] Laboratoire de Chimie Théorique et Physico-Chimie Moléculaire-UMR 5624, Université de Pau, France
[4] Physics Department, Indian Institute of Technology, Roorkee (Uttaranchal) 247667, India
[5] Computational Materials Science Laboratory, Physics Department, University of Sidi-Bel-Abbès, Algeria

Received 27 January 2005 / Received in final form 31 March 2005
Published online 21 September 2005 –

Abstract. A theoretical study of structural, elastic, electronic and optical properties of CaF_2, SrF_2 and BaF_2 is presented, using the full-potential linearized augmented plane-wave (FPLAPW) method as implemented in the Wien97 code. In this approach the generalized gradient approximation (GGA) was used for the exchange-correlation (XC) potential. Results are given for lattice constant, bulk modulus, its pressure derivative and elastic constants. Band structure, density of states, pressure coefficients of energy gaps and refractive indices are also given. The results are compared with previous calculations and experimental data.

PACS. 71.15.Mb Density functional theory, local density approximation, gradient and other corrections – 71.15.-m Methods of electronic structure calculations – 62.20.Dc Elasticity, elastic constants – 78.20.-e Optical properties of bulk materials and thin films

1 Introduction

Recently, it has become possible to compute with a great accuracy an important number of electronic and structural parameters of solids from first-principles calculations. This kind of development in computer simulations has opened up many interesting and existing possibilities in condensed matter studies. For example, it is now possible to explain and to predict properties of solids which were previously inaccessible to experiments.

The fluorite crystal structure (C1) is a common to many interesting materials. Among them the compounds of fluorine with divalent metal halides AF_2 (A = Ca, Sr, Ba, Pb) constitute a family of fluorite type-crystals [1]. These compounds are highly ionic insulators with a large band gap, crystallizing at ambient conditions in the cubic fluorite structure [2–5]. These compounds have been extensively studied experimentally for their intrinsic optical properties [6–23]. There exist also, other studies for these alkaline fluorides. Diffuse phase transition studies in cubic fluorite type BaF_2 were performed by Oberschmidt [24] and Catlow et al. [25]. Pressure induced color centers in CaF_2 and BaF_2 was studied by Minomura and Drickamer [26]. The supra-iconicity studies in alkaline earth fluoride CaF_2, BaF_2 and SrF_2 have been done by Zhon et al. [27], using molecular dynamic simulations. The ionic conductivity studies of CaF_2, SrF_2, BaF_2 and $SrCl_2$ have performed at high temperatures by Voronin and Volkov [28]. The crystal structure and binding in the $PbCl_2$ structure of CaF_2 compound have been studied by Elaine et al. [29] using the X-ray diffraction.

From a theoretical point of view, several first principles calculations were made for CaF_2, SrF_2 and BaF_2 compounds by a variety of methods [30–51]. Starostin et al. [30,31] have used the tight binding (TB), orthogonalized-plane-wave (OPW) and the augmented plane wave method (APW) methods to calculate the band structure of CaF_2 compound. Albert and Jouanin [32,33], and Heaton and Lin [34] reported some band structure results on CaF_2 compound. These authors used the self-consistent linear combination of atomic orbital (LCAO) method for the valence bands and the OPW method for the conduction bands. In the beginning of 90's, Kudrnovsky et al. [35] have studied the electronic structure of fluorite type crystals CaF_2, SrF_2, CdF_2 and PbF_2 by means of the linear muffin-tin-orbital (LMTO) method.

[a] e-mail: mohammed.sahnoun@unifr.ch

The DFT-LCAO method have used by Catti et al. [36] to discuss the band structure of CaF_2. The gradient self-consistent orthogonalized OLCAO method has been used by Ching and co-workers [37,38] to discuss the band structure and the related properties such as the optical properties of these compounds.

Recently, Kootstra et al. [39] have studied the dielectric function of CaF_2, SrF_2 and BaF_2 compounds by means of real space and full potential dependent density functional theory. Kanchana et al. [40–42] have presented the electronic structure and high pressure phase transition of these compounds, using the TB-LMTO method. Jiang et al. [43] have calculated the structural, electronic and optical properties of BaF_2 compound in its stable (cubic) and high pressure phases, using a self consistent DFT-LCAO. The electronic structure, dielectric and vibrationnal properties have been determined by Verstraete and Gonze [44], using the DFT. The optical properties have been studies by Burnett et al. [45], Benedict and Shirley [46], using the Hartree-Fock-Pseudopotentials enhanced by core polarization potentials, and in particular the intrinsic quality of the birefringence in CaF_2 at short wavelengths. On a side note, de Leeuw et al. [47,48] studied the effect of water on the surface of CaF_2.

The elastic constants of CaF_2 crystal have been calculated more than ten years ago by Catti et al. [36] and by Martin-Pendas et al. [49], using the Hartree-Fock level of theory and the quantum-mechanical ab initio perturbedion (AIPI) model, respectively. Very recently, two of the mentioned ab initio studies [50,51] discuss calculations of the elastic constants of the alkaline earth fluorite CaF_2, SrF_2 and BaF_2.

From the above it is clear that there exist many band structure calculations for these compounds. Photoelastic constants have been analyzed [50] for the three fluorides, but no earlier calculations appear to study the effect of the hydrostatic pressure on the band structure or imaginary part of the dielectric constant above the band gap. We note that all the calculations are based on the muffin-tin approximation. We would therefore be worthwhile to do more accurate calculations based on full potential methods. In this paper we use the full potential LAPW method to calculate the band structure, elastic constants, density of states, optical properties and the effect of the hydrostatic pressure on the electronic and optical properties.

The rest of the paper is organized as follows: in Section 2, we briefly describe the computational techniques used in this work. Results and discussion of the structural, elastic, electronic and optical properties will be presented in Section 3. Finally, we present a brief conclusion.

2 Calculation method

The first-principles calculations are performed by employing FPLAPW approach [52,53] based on DFT [54] and implemented in Wien97 [55] code. The Kohn-Sham equations are solved self-consistently using FPLAPW method. In the calculations reported here, we use a parameter $R_{\mathrm{MT}}K_{\max} = 8$, which determines matrix size (convergence), where $K_{\max}$ is the plane wave cut-off and R_{MT} is the smallest of all atomic sphere radii. We have chosen the muffin-tin radii (MT) for Ca, Sr and Ba to be 2.3, 2.5 and 2.8 a.u., respectively in CaF_2, SrF_2 and BaF_2. We used $R_{\mathrm{MT}} = 2.2$ a.u. for fluorine atoms in these compounds. Exchange-correlation (XC) effects are treated by GGA [56]. The self-consistent calculations are considered to be converged when the total energy of the system is stable within 10^{-4} Ry. The integrals over the Brillouin zone are performed up to 16 k-points in the irreducible Brillouin zone, using the Monkhorst-Pack special k-points approach [57].

For the calculations of the optical properties, a dense mesh of uniformly distributed k-points is required. Hence, the Brillouin zone integration was performed with 47 and 104 points in the irreducible part of the Brillouin zone with broadening. We find a very small difference in the two calculations. We present calculations with only 47 points in this paper. The frequency dependent complex dielectric function $\varepsilon(\omega) = \varepsilon_1(\omega) + i\varepsilon_2(\omega)$ is known to describe the optical response of the medium at all photon energies $E = \hbar\omega$. The imaginary part of the $\varepsilon(\omega)$ in the long wavelength limit has been obtained directly from the electronic structure calculation, using the joint density of states (JDOS) and the optical matrix elements. The real part of $\varepsilon(\omega)$ can be derived from the imaginary part by using the Kramers-Krönig relationship. The knowledge of both the real and imaginary parts of $\varepsilon(\omega)$ allows the calculations of important optical functions. In this paper, we also present and analyze the real part of refractive index $n(\omega)$, given by:

$$n(\omega) = \left[\frac{\varepsilon_1(\omega)}{2} + \frac{\sqrt{\varepsilon_1^2(\omega) + \varepsilon_2^2(\omega)}}{2}\right]^{1/2}. \quad (1)$$

At low frequency ($\omega = 0$), we get the following relation:

$$n(0) = \varepsilon^{\frac{1}{2}}(0). \quad (2)$$

3 Results and discussion

The total energies are computed for specified sets of lattice constants. Our data results from the best fit obtained with the Murnaghan equation of state [58] built up 12 points, in the range $V_{\mathrm{equ}}(1 \pm 0.05)$ (V_{equ} is the equilibrium volume of the unit cell). The computed equilibrium lattice constants are 5.515, 5.856, 6.233 Å for CaF_2, SrF_2 and BaF_2, respectively. From these fits, we have also calculated the bulk moduli to be 82.14, 68.8, and 56.4 GPa, and their pressure derivatives to be 3.68, 3.42, 3.38 for CaF_2, SrF_2 and BaF_2, respectively. In Table 1 we summarize our data at the equilibrium in the fluorite-C1 phase and compare them with the experimental data and with the previous calculations using GGA-LCAO method (for CaF_2, SrF_2 and BaF_2; see [43,51]), the LDA-TB-LMTO (for CaF_2, SrF_2; see [42] and for BaF_2; see [41]), the LDA-OLCAO (for CaF_2, SrF_2 and BaF_2; see [37]), the ab initio

Table 1. Calculated lattice constant (in Å), bulk modulus (in GPa), pressure derivative (B') compared to experimental data and other works of CaF_2, SrF_2 and BaF_2 for C1-fluorite phase.

	Lattice constant (Å)	B (GPa)	B'
CaF_2			
Present	5.515	82.14	3.68
Expt.	5.46[a]	84.1[b]	4.92[b]
	5.44[c]	84.7[d]	
GGA-LCAO[e]	5.513	79.5	
LDA-OLCAO[f]	5.46		
LDA-TBLMTO[g]	5.34	103	
AIPI[h]	5.444	82.7	4.0
PAIRPOT[h]	5.563	84.7	4.2
LDA-PP[i]	5.464		
SrF_2			
Present	5.856	68.8	3.42
Expt.	5.80[a]	69.0[j]	
GGA-LCAO[e]	5.887	61.6	
LDA-OLCAO[f]	5.80		
LDA-TBLMTO[g]	5.64	90.35	
LDA-PP[i]	5.796		
BaF_2			
Present	6.233	56.4	3.38
Expt.	6.20[a,k]	57.0[k]	4.00[k]
GGA-LCAO	6.292[l]	57.3[l]	4.91[l]
	6.32[e]	58.5[e]	
LDA-OLCAO[f]	6.20		
LDA-TBLMTO[m]	6.08	79.64	
LDA-PP[i]	6.196		

[a] [59]; [b] [60]; [c] [61];
[d] [62]; [e] [51]; [f] [37];
[g] [42]; [h] [49]; [i] [50];
[j] [5]; [k] [4]; [l] [43]; [m] [41].

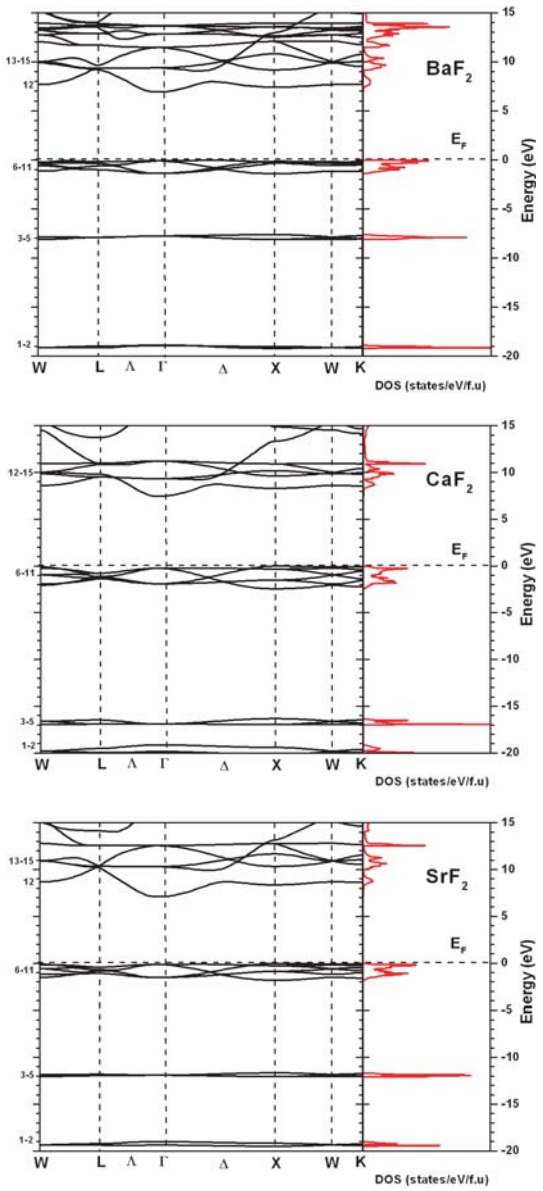

Fig. 1. The band structures (left panel) and density of states (right panel) of BaF_2, CaF_2 and SrF_2.

perturbed ion (AIPI) and the pair interaction model implemented in a computational code called PAIRPOT (for CaF_2; see [49]) and the LDA-Pseudopotential (PP) (for CaF_2, SrF_2 and BaF_2; see [50]). Our calculated structural parameters show very good agreement with the theoretical [37,43,49–51] and experimental data [4,5,59–61]. The small overestimation in the equilibrium lattice constants is a common feature with GGA calculations. To verify the accuracy of these results, several tests have been performed using different muffin tin radius as well as different sets of special k-point to ensure the convergence.

We have also calculated the elastic constants (C_{11}, C_{12} and C_{44}) for the three compounds using the method discussed in detail in reference [63], and our previous papers for the SrX compounds [64] and the alkaline earth oxides [65]. In Table 2 we compare our calculated elastic constant with the theoretical [50,51] and experimental data [25,62,66,67]. Our calculated values of C_{11} for CaF_2 and SrF_2, are significantly smaller than the experimental data. However, our results are in reasonable agreement with the experimental results and other calculations.

The calculated electronic-band structures for the fluorite phase along the various symmetry lines are given in Figure 1 (right panel) for CaF_2, SrF_2 and BaF_2 compounds. The overall band profiles are found to be the same for the three compounds and are in good agreement with other band structures [35,37,38,41–43]. In the absence of the spin orbit interaction (our calculations), the top of the valence band (VB) is found at X point in CaF_2 and SrF_2 compounds, while in BaF_2 the top is found along the Δ direction. The fluorine s states appear at about 16.95, 19.42 and 19.15 eV below the top of the VB in CaF_2, SrF_2 and BaF_2, respectively. The barium s states appear at about 22.66 eV below the top of the VB. In these compounds,

Table 2. Calculated elastic constants Cij compared to experimental data and other works of CaF_2, SrF_2 and BaF_2 for the C1 phase. All of the pressures are in GPa.

		Calc.			Expt.		
		Present	GGA-LCAO[a]	LDA- PP[b]	BS[c]	US	US'
CaF_2							
	C_{11}	146.13	158.5	183	165.5 ± 2.5	165.07[d]	173.0[c]
	C_{12}	50.17	39.7	61	38.9 ± 0.7	44.51[d]	40.5[c]
	C_{44}	43.18	35.1	34	33.5 ± 2.0	33.83[d]	37.5[c]
SrF_2							
	C_{11}	97.20	121.1	135	123.8 ± 1.9	123.46[e]	128.8[e]
	C_{12}	54.6	40.5	54	42.6 ± 0.7	43.06[e]	47.50[e]
	C_{44}	35.31	30.1	31.6	32 ± 2	31.28[e]	33.08[e]
BaF_2							
	C_{11}	90.14	92.6	110.33	91.7 ± 1.4	89.15[f]	98.10[f]
	C_{12}	39.53	40.2	54.33	39.5 ± 0.6	40.02[f]	44.81[f]
	C_{44}	25.02	21.72	27.4	25.1 ± 0.9	25.35[f]	25.44[f]

[a] [51]; [b] [50]; [c] [25]; [d] [62]; [e] [66]; [f] [67].

the upper VB, which is lying close to the Fermi level, are dominated by the p states of the fluorine atoms. In these compounds, the conduction band (CB) have compounds primarily from the d states with a few contribution of s states of the metal atoms and the bottom of band occurs at Γ point making the compounds to have an indirect band gap insulators of about 7.45, 7.12, 6.97 eV for CaF_2, SrF_2 and BaF_2, respectively.

The results of our calculations are in agreement with the earlier calculations for the conduction band configuration, predicting the conduction band minimum (CBM) at Γ point. However the agreement disappears when we consider the VB configuration. Our calculations, along with the TB-LMTO and the first principles self-consistent OLCAO calculations, show a valence band maximum (VBM) at X point, predicting that CaF_2 is an indirect band gap material (X–Γ) with a gap of 7.24 and 6.53 eV, respectively. Our calculated band gap for CaF_2 compound is much smaller than the one obtained by experiment (12.1 eV), and those derived from theory, which are namely 9.8 and 11.38 eV. The former value was determined by the full Slater exchange and their self-consistent calculations, whereas the later one by the GW-calculations [68]. This discrepancy is due to the fact that LDA Kohn-Sham states do not take into account the quasiparticle self energy correctly [69]. Our results for SrF_2 and BaF_2 compounds are in disagreement with the TB-LMTO and LCAO calculations. The upper VB occurs at Z-point predicting that SrF_2 and BaF_2 are indirect-band-gap materials (Z-Γ) with gaps of 7.55 and 7.033 eV for SrF_2 and BaF_2, respectively [42]; while the highest VB occurs at Γ point predicting that BaF_2 is a direct band gap (Γ–Γ) with a gap of 7.49 eV [43].

The density of states (DOS) of these fluorides is presented in Figure 1 (left panel). The behavior of our calculated DOS of CaF_2 and BaF_2 is similar to those obtained by OLCAO calculations for CaF_2 (see [38]) and LCAO calculations for BaF_2 (see [70]). Analysis of the width of peaks from these DOS, give a bandwidth of the upper VB equal to 2.45 eV for CaF_2. For this compound, the Hartree-Fock calculations and the experimental measurements determine a total width of the upper VB of about 3.1 eV [16,38]. This experimental value is smaller of about 0.39 eV than that found by Shirley [68] using GW-calculations. According to the suggestion of Himpsel and co-workers, which state that the earlier results of the band gap from photoemission are probably in error [71], and consequently the GW results are more realistic. Other calculations gave somewhat narrower VB widths (2.0 eV by Heaton and Lin [34] and 2.7 eV by Albert et al. [33]).

To our knowledge, there are no photoemission studies in SrF_2 and BaF_2 available to make meaningful comparison with the calculated valence bandwidths. We find the upper valence bandwidth of 1.84 eV and 1.40 eV for SrF_2 and BaF_2, respectively. The self consistent field approach based on the HF approximation LCAO calculations [70] finds a width of 1.96 eV for BaF_2 compound. The deviation between our results and other theoretical ones, seems to be due to differences between the methodologies used in the calculations.

It is well known that the GW-calculations give energy band gaps in excellent agreement with experiment, as shown by Shirley [68] for CaF_2 compound. It is important to note that the density functional formalism is limited in its validity (see [72]) and the band structure derived from it cannot be used directly for comparison with GW-calculations.

The GGA within the density functional formalism does not accurately describe the eigenvalues of the electronic states, which causes quantitative underestimations of band-gaps compared with experiment. However, despite this shortcoming of the GGA, the pressure derivatives or the deformation potentials of band gaps are accurately calculated in the GGA (or LDA) and do not depend on

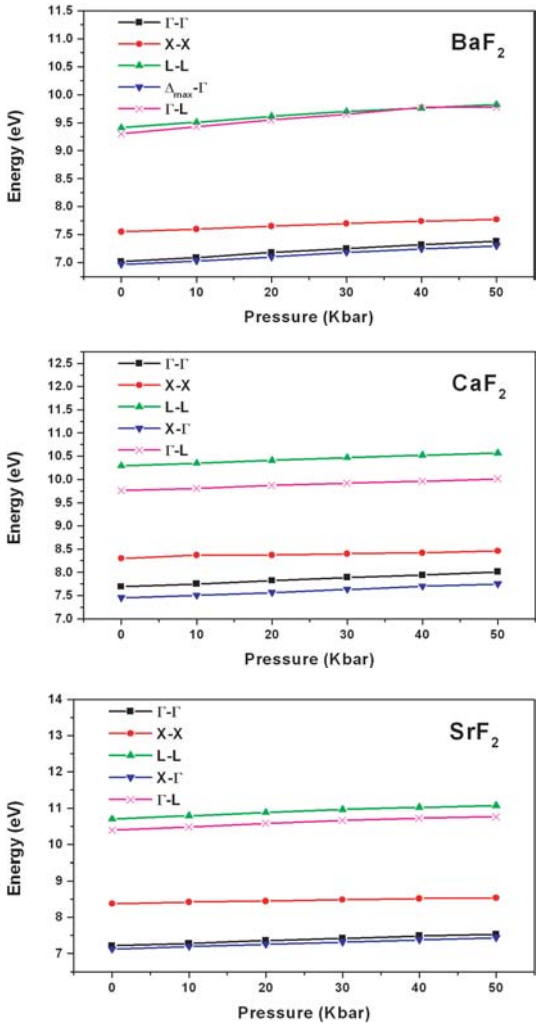

Fig. 2. Calculated dependence of the band gaps of BaF_2, CaF_2 and SrF_2 on the change in pressure.

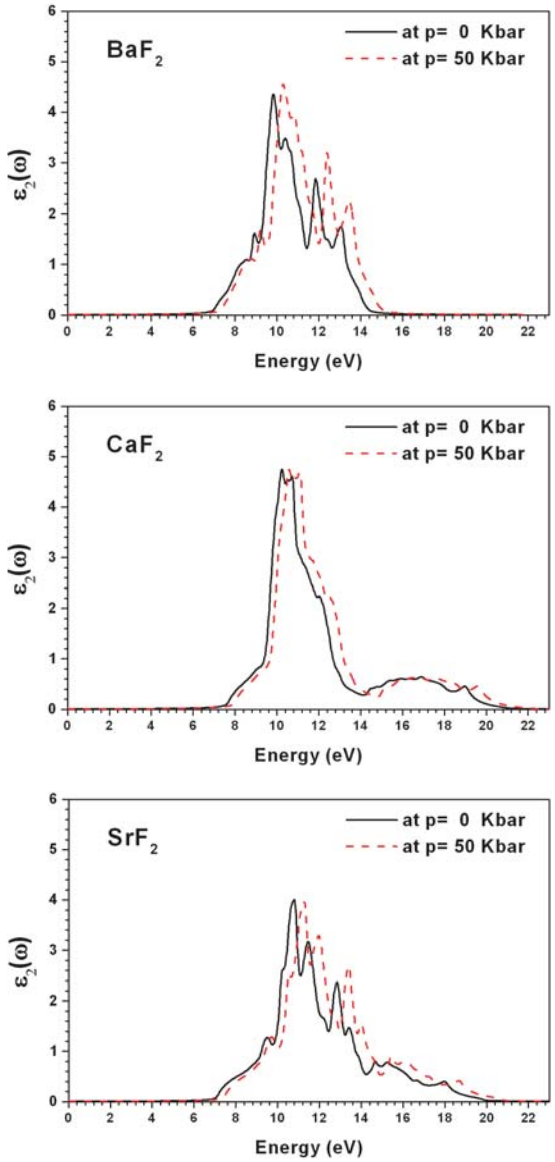

Fig. 3. Imaginary part of the dielectric function of BaF_2, CaF_2 and SrF_2.

the type or functional form of the exchange-correlation potential [73–75]. As such we have investigated the effect of the pressure on the size of the energy gap and position of the minimum of the conduction band for the three compounds CaF_2, SrF_2 and BaF_2. Results of our calculations for the direct and indirect band gaps for these materials versus the pressure are shown in Figure 2. We notice that these compounds have an indirect gap ((X–Γ) for CaF_2 and SrF_2 and ($\Delta_{\max}$–Γ) for BaF_2) at equilibrium volume. We can remark that the fundamental gaps (X–Γ) and ($\Delta_{\max}$–Γ) increase under hydrostatic pressure. We can also note that the fundamental gaps and other ones (Γ–Γ, X–Γ, X–X, Γ–L) seem to have a linear behavior. However, the behavior of these energy gaps is not so linear versus the pressure, as it can be seen, particularly for theses compounds, where a strong sub-linear behavior is found between pressure and gaps along (Γ–L) transition for SrF_2 and BaF_2 compared to that of the direct and indirect gaps (Γ–Γ), (X–X) and (X–Γ). The calculated linear and quadratic pressure coefficients are listed for different gaps in Table 3. The linear and quadratic pressure coefficients increase with the increase of cationic atoms. Concerning BaF_2 compound, our calculated linear pressure along (Γ–Γ) and (X–X) directions are relatively close to those of [43] obtained by the LCAO method within the GGA level. We are not aware of experimental data to compare with our results. We can consider the present results of linear and quadratic pressure coefficients as a prediction study.

Figure 3 shows the variation of the imaginary (absorptive) part of the electronic dielectric function ε_2 at normal and under hydrostatic pressure within GGA approximation for CaF_2, SrF_2 and BaF_2, for radiation up to 20 eV. As can be seen the linear optical absorption varies from a compound to another. This is attributed to the conduction bands that are usually quite different, and to the symmetries of the wave functions which dictate that the selection rules are fully reflected in the Matrix Moment

Table 3. Calculated linear and quadratic pressure coefficients of important band gap for CaF_2, SrF_2, and BaF_2 compounds in fluorite C1 phase. $E_i(p) = E_i(0) + bp + \frac{1}{2}cp^2$, $b = \partial E_i/\partial p$ in eV $\times 10^{-2}$ GPa^{-1}, $c = \partial^2 Ei/\partial p^2$ in eV $\times 10^{-3}$ GPa^{-2}.

	Γ–Γ		X–X		Γ–L		Δ_{max}–Γ		X–Γ	
	b	c	b	c	b	c	b	c	b	c
CaF_2	6.67	–1.07	3.42	–2.5	5.71	–2.85	–	–	5.84	–1.43
SrF_2	7.65	–5.0	4.15	–3.57	11.23	–14.64	–	–	6.85	–1.78
BaF_2	8.48	–4.64	5.74	–5.0	15.41	–21.42	7.1	–1.43	8.43	–0.37
	9.10[a]		2.68[a]		11.61[a]				7.45[a]	

[a]Reference [43].

Elements (MME's). The real part of the dielectric function $\varepsilon_1$was also obtained by Kramers-Kronig conversion but are not shown. There is an overall topological resemblance of the present $\varepsilon_2(\omega)$ curves and those calculated by the OLCAO method [37,38]. Especially, the corresponding positions of the major peaks in $\varepsilon_2(\omega)$ curve for CaF_2 compound are found at 9.95, 10.27, 11.01, 12.02 and 19.12 eV, while Gan et al. [38] find these peaks at 14, 14.6, 15.5, 16.2 and 25.2 eV with an applied shift of 4.2 eV.

Using our calculated band structures (Band 1 has been indexed starting from the lowest energy) it would be worthwhile to identify the interband transitions that are responsible for the structures in $\varepsilon_2(\omega)$. Our analysis of the $\varepsilon_2(\omega)$ curves show that the threshold peaks appear at 7.69 eV in CaF_2, 7.22 eV in SrF_2 and 7.02 eV in BaF_2. These energies are related to direct transitions $\Gamma_{11} \rightarrow \Gamma_{12}$. Under pressure the values of the threshold peaks increase, as a consequence of the increase in direct band gaps in band structures. In these compounds there are two groups of peaks. The first one is situated from 8.0 to 10.0 eV, 10.60 eV and 9.45 eV for CaF_2, SrF_2 and BaF_2, respectively. These groups of peaks are related to direct transitions along W–L and W–K directions for CaF_2 and SrF_2 and along W–L, Δ and Λ directions for BaF_2. In these groups we find pronounced peaks localized at 9.95 eV in CaF_2, 9.50 and 10.24 eV in SrF_2, and at 8.50 and 8.91 in BaF_2. These peaks are related to direct transitions W_6–W_8 and along W_6–K_{14} direction in CaF_2. In SrF_2 compound, the first pronounced peak is related to the direct transitions along X_3–W_7 direction and the second one is related to the direct transition along W_1–L_7 direction. In BaF_2 compound, the first peak is related to the direct transition along W_5–L_7 direction and the second one is related to the direct transition along Γ_1–X_7 and W_1-L_7 directions. Our results on the location of the first peaks and their origin in BaF_2 compound are in disagreement with the experimental and theoretical studies. For example, the first peak was reported to be at 10, 11 and 12 eV in reflectance [13], characteristic energy loss [7], and XPS measurements [14], respectively. Theoretically, Jiang et al. [43] assigned the interband transition from the top of the valence band and the bottom of the conduction band at Γ to the first peak and that one at X to the second peak. The main peaks in the spectra of CaF_2, SrF_2 and BaF_2 are situated at 10.27, 10.87 and 9.87 eV respectively. These peaks are related to the direct transitions $\Gamma_6 \rightarrow \Gamma_9$ and $\Gamma_6 \rightarrow \Gamma_8$ for CaF_2, along W_5–K_8 and W_5–X_8 directions for SrF_2 and along X_5–W_8, W_5–L_8, Γ_5–X_8 directions for BaF_2. The second group of peaks (10.30–15 eV in CaF_2, 11−16 eV in SrF_2 and 10–14 eV in BaF_2) comes from the direct transitions along the X_2–W_7, W_1–L_7, W_4–L_{10}, X_4–W_6, K_4–K_6 and W_2–K_{10} directions in CaF_2, along the W_5–L_{10}, W_2–W_{10} and W_2–L_{10} directions in SrF_2 and along W_6–L_{10}, W_2–L_{10}, Λ, X_2–W_{10}, Δ directions in BaF_2.

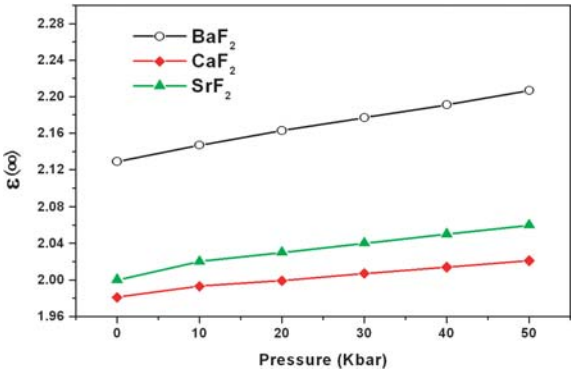

Fig. 4. Pressure dependence of $\varepsilon(\infty)$ of BaF_2, CaF_2 and SrF_2.

Figure 4 shows the calculated results for the pressure dependence of the static electronic constant $\varepsilon(\infty)$ for CaF_2, SrF_2 and BaF_2 in the GGA approximation obtained from relation (2). As can be seen the increase of the dielectric constants (refractive index) with pressure is practically linear in all the compounds. The pressure derivative of the refractive index n of CaF_2, SrF_2 and BaF_2 are determined by a polynomial fit. Our calculated pressure and volume coefficients of refractive index are also listed in Table 4. From this table, we can also notice that the calculated dielectric constant and pressure coefficient values increase with the increase of the size of the cation atoms. There are no experimental or theoretical results for the variation under pressure of the refractive indices available to us for these compounds. We can consider the present results of the linear pressure and volume coefficients as a prediction study for these compounds, and hence will stimulate some other works on these materials.

Table 4. The calculated dielectric constants $\varepsilon(\infty)$, pressure and volume coefficients of refractive index for CaF_2, SrF_2 and BaF_2.

Compounds	$\varepsilon(\infty)$			$\frac{1}{n_0}\frac{dn}{dp}(10^{-3}\mathrm{GPa}^{-1})$	$\frac{v_0}{n_0}\frac{dn}{dv}$
	Present	Expt.	Other works		
CaF_2	1.981	2.04[a]	1.49[a], 2.02[d]	1.944	–0.18
		1.50[b,c]			
SrF_2	2.00	2.06[a]	1.12[a]	2.834	–0.226
BaF_2	2.129	2.15[a]	1.07[a], 2.012[e]	3.564	–0.24

[a] [37]; [b] [15]; [c] [76]; [d] [38]; [e] [43].

4 Conclusion

In conclusion, we have used GGA within the FPLAPW method to study the electronic and optical properties at normal and hydrostatic pressure of the cubic alkaline fluorides CaF_2, BaF_2 and SrF_2. The critical point structure of the frequency dependent complex dielectric function was investigated and analyzed to identify the optical transitions. We have compared our results of structural parameters, elastic constants and refractive dielectric constants with the previous calculations using different methods. In particular, good agreement is found with the GGA study of these compounds ([43,51] using LCAO crystalline orbital (Program CRYSTAL [77]), the TB-LMTO [41,42] and the OLCAO [37,38]. There appear to be no earlier studies of the effect of hydrostatic pressure on the band structure or imaginary part of the dielectric constant above the band gap, so our calculations can be used to cover this lack of data for these compounds.

References

1. W. Pics, A. Weiss, in *Crystal Structure of Inorganic Compounds: Keys Elements F, Cl, Br, I*, edited by K.H. Hellwege, A.M. Hellwege, Landolt-Börnstein, New series, Vol. III/7a (Springer, Berlin, 1973)
2. L. Gerward, M. Malinowski, S. Asbrink, A. Waskowska, J. Appl. Cryst. **25**, 1584 (1992)
3. R.M. Hazen, L.W. Finger, J. Appl. Cryst. **14**, 234 (1981)
4. J.M. Leger, J. Haines, A. Atouf, O. Schulte, S. Hull, Phys. Rev. B **52**, 13247 (1995)
5. G.A. Samara, Phys. Rev. B **13**, 4529 (1976)
6. W. Hayes, A.B. Kunz, E.E. Koch, J. Phys. C **4**, L200 (1971)
7. J. Frandon, B. Lahaye, F. Pradal, Phys. Status Solidi B **53**, 565 (1972)
8. C. Sánchez, M. Cardona, Phys. Status Solidi B **50**, 293 (1972)
9. A. Feldman, R.M. Waxler, Phys. Rev. Lett. **45**, 126 (1980)
10. O.V. Shakin, M.F. Bryzhina, V.V. Lamanov, Sov. Phys. Solid State **13**, 3141 (1972)
11. M.M. Elcombe, A.W. Pryor, J. Phys. C **3**, 492 (1970)
12. A.K. McCurdy, Phys. Rev. B **26**, 6971 (1982)
13. G.W. Rubloff, Phys. Rev. B **5**, 662 (1972)
14. M. Scrocco, Phys. Rev. B **32**, 1301 (1985)
15. J. Barth, R.L. Johenson, M. Cardona, Phys. Rev. B **41**, 3291 (1990)
16. R.T. Poole, J. Szajman, R.C.G. Leckey, J.C. Jenkin, J. Liesegang, Phys. Rev. B **12**, 5872 (1975)
17. I. Hernández, F. Rodríguez, Phys. Rev. B **67**, 012101-1 (2003)
18. S.C. Sabharwal, Sangeeta, A.K. Chauhan, J. Cryst. Growth **240**, 473 (2002)
19. Y. Gao, T. Tiedje, P.C. Wong, K.A.R. Mitchell, Phys. Rev. B **48**, 15578 (1993)
20. T. Tsujibayashi, M. Watanabi, O. Arimoto, M. Itoh, S. Nakanishi, H. Itoh, S. Asaka, M. Kamada, Phys. Rev. B **60**, R8442 (1999)
21. B. Wang, Solid State Technol. **43**, 77 (2000)
22. R. Gupta, J.H. Burnett, U. Griesmann, M. Walhout, Appl. Opt. **37**, (5964) 1998
23. J.H. Burnett, R. Gupta, U. Griesmann, Appl. Opt. **41**, 2508 (2002)
24. J. Oberschmidt, Phys. Rev. B **23**, 5038 (1991)
25. C.R.A. Catlow, J.D. Comins, F.A. Germano, R. Tharley, W. Hayes, J. Phys. C **11**, 3197 (1978)
26. S. Minomura, H.G. Drickamer, J. Chem. Phys. **34**, 670 (1961)
27. L.X. Zhon, J.R. Herdy, H.Z. Cao, Solid State Commun. **98**, 341 (1996)
28. B.M. Voronin, S. Volkov, J. Phys. Chem. Solids **62**, 1349 (2001)
29. M. Elaine, G. Tom, L. Kurt, J. Phys. Chem. Solids **62**, 1117 (2001)
30. N.V. Starostin, V.A. Ganin, Fiz. Tverd. Tela **15**, 3404 (1973); N.V. Starostin, V.A. Ganin, Sov. Phys. Solid-State **15**, 2265 (1974)
31. N.V. Starostin, M.P. Shepilov, Fiz. Tverd. Tela **17**, 882 (1975); Sov. Phys. Solid-State **17**, 523 (1975)
32. J.P. Albert, C. Jouanin, C. Cout, Phys. Rev. B **16**, 4619 (1977)
33. J.P. Albert, C. Jouanin, C. Cout, Phys. Rev. B **16**, 925 (1977)
34. R.A. Heaton, C.C. Lin, Phys. Rev. B **22**, 3629 (1980)
35. J. Kudrnovský, N.E. Christensen, J. Mašek, Phys. Rev. B **43**, 12597 (1991)
36. M. Catti, R. Dovesi, A. Pavese, R. Saunders, J. Phys.: Condens. Matter **3**, 4151 (1991)
37. W.Y. Ching, F. Gan, M.-Z. Huang, Phys. Rev. B **52**, 1596 (1995)
38. F. Gan, Y.-N. Xu, M.-Z. Huang, W.Y. Ching, Phys. Rev. B **45**, 8248 (1992)
39. F. Kootstra, P.L. de Boeij, J.C. Snijders, Phys. Rev. B **62**, 7071 (2000)
40. V. Kanchana, G. Vaitheeswaran, M. Rajagopalan, J. Alloy Compd. **352**, 60 (2003)

41. V. Kanchana, G. Vaitheeswaran, M. Rajagopalan, J. Alloy Compd. **359**, 66 (2003)
42. V. Kanchana, G. Vaitheeswaran, M. Rajagopalan, Physica B **328**, 283 (2003)
43. H. Jiang, R. Pandey, C. Darrigan, M. Rérat, J. Phys.: Condens. Matter **15**, 709 (2003)
44. M. Verstraete, X.Gonze, Phys. Rev. B **68**, 195123 (2003)
45. J.H. Burnett, Z.H. Levine, E.L. Shirley, Phys. Rev. B **64**, 241102 (2001)
46. L.X. Benedict, E.L. Shirley, Phys. Rev. B **59**, 5441 (1999)
47. N.H. de Leeuw, J.A. Purton, S.C. Parker, G.W. Watson, G. Kresse, Surf. Sci. **425**, 9 (2000)
48. N.H. de Leeuw, T.G. Cooper, J. Mater. Chem. **13**, 93 (2003)
49. A. Martin Pendás, J.M. Recio, M. Flórez, V. Luaña, M. Bermejo, Phys. Rev. B **49**, 5858 (1994)
50. Z.H. Levine, J.H. Burnett, E.L. Shirley, Phys. Rev. B **68**, 155120 (2003)
51. M. Mérawa, M. Llunell, R. Orlando, M.G. Duvignau, R. Dovesi, Chem. Phys. Lett. **368**, 7 (2003)
52. P. Blaha, K. Schwarz, P. Sorantin, S.B. Trickey, Comput. Phys. Commun. **59**, 399 (1990)
53. D.J. Singh, *Plane Waves, Peudopotential and the LAPW Method* (Kluwer Academic Publishers, Boston, Dortrecht, London, 1994)
54. P. Hohenberg, W. Kohn, Phys. Rev. B **136**, 864 (1964)
55. P. Blaha, K. Schwarz, J. Luitz, Wien'97, Vienna University of Technology, Improved and Updated Unix Version of the original Copyrighted WIEN-code, Which was published in: P. Blaha, K. Schwarz, P. Sorantin, S.B. Trickey. Comput. Phys. Commun. **59**, 399 (1990)
56. J.P. Perdew, K. Burke, M. Ernzerhof, Phys. Rev. Lett. **77**, 3865 (1996)
57. H.J. Monkhorst, J.D. Pack, Phys. Rev. B **13**, 5188 (1976)
58. F.D. Murnaghan, Proc. Natl. Acad. Sci. USA **30**, 244 (1944)
59. R.W.G. Wyckoff, Crystal structures, 2nd edn. **1** (Interscience Publisher, New York, 1982)
60. C. Wang, D.E. Schuele, J. Phys. Chem. Solids **29**, 1309 (1968)
61. G.K. White, J. Phys. C **13**, 4905 (1980)
62. P.S. Ho, A.L. Ruoff, Phys. Rev. **161**, 864 (1967)
63. M.J. Mehl, Phys. Rev. B **47**, 2493 (1993)
64. R. Khenata, H. Baltache, M. Rérat, M. Driz, M. Sahnoun, B. Bouhafs, B. Abbar, Physica B **339**, 208 (2003)
65. H. Baltache, R. Khenata, M. Sahnoun, M. Driz, B. Abbar, B. Bouhafs, Physica B **344**, 334 (2004)
66. D. Gerlich, Phys. Rev. A **135**, 1331 (1966)
67. D. Gerlich, Phys. Rev. A **136**, 1366 (1964)
68. E.L. Shirley, Phys. Rev. B **58**, 9579 (1998)
69. S.N. Rashkeev, W.R.L. Lambrecht, Phys. Rev. B **63**, 165212 (2001)
70. A.B. Sobolev, A.Yu. Kuznetsov, J. Andriessen, C.W.E. Van Eijk, Nucl. Instrum. Meth. A **486**, 385 (2002)
71. F.J. Himpsel, L.J. Terminello, D.A. Lapiano-Smith, E.A. Eklund, J.J. Barton, Phys. Rev. Lett. **68**, 3611 (1992)
72. G. Onida, L. Reining, A. Rubio, Rev. Mod. Phys. **74**, 601 APR (2002)
73. X.J. Zhu, S. Fahy, S.G. Louis, Phys. Rev. B **39**, 7840 APR15 (1989)
74. S.H. Wei, A. Zunger, Phys. Rev. B **60**, 5404 (1999)
75. B. Bouhafs, H. Aourag, M. Certier, J. Phys.: Condens. Matter **12**, 5655 (2000)
76. G. Stephan, Y. le Calvez, J.C. Lemonier, S. Robin, J. Phys. Chem. Solids **30**, 601 (1969)
77. R. Dovesi, V.R. Saunders, C. Roetti, M. Causà, N.M. Harisson, R. Orlando, E. Aprà, CRYSTAL95 User's Manual (Universidad de Torino, Torino, 1996)